A multi-century meteo-hydrological analysis for the Adda river basin (Central Alps). Part I: gridded monthly precipitation (1800–2016) records

Alice Crespi[1,*], Michele Brunetti[2], Roberto Ranzi[3], Massimo Tomirotti[3], Maurizio Maugeri[1,2]

[1]*Department of Environmental Science and Policy, Università degli Studi di Milano, Milan, 20133, Italy*

[2] *Institute of Atmospheric Sciences and Climate, ISAC-CNR, Bologna, 40129, Italy*

[3]*DICATAM, Università degli Studi di Brescia, Brescia, 25123, Italy*

[*] *Now at the Institute for Earth Observation, Eurac Research, Bolzano, 39100, Italy*

Corresponding author: Alice Crespi, email: alice.crespi@eurac.edu, phone: +39 3477777563

Running head: A multi-century monthly precipitation record for Adda basin

Keywords: anomaly method, secular precipitation, long-term trend, runoff comparison

This research received no specific grant from any funding agency in the public, commercial or not-for-profit sectors.

Abstract

The 1800–2016 monthly precipitation record for the upper Adda river basin is presented. It is computed by applying the anomaly method to a quality-checked and homogenized observation database. The reconstruction accuracy and its evolution over the study period is evaluated at both station and grid-cell levels. The anomaly-based interpolation provides rather robust estimates even for the early years of sparse station coverage with basin precipitation reconstruction errors around 10%. The Theil-Sen trend analysis on the basin precipitation series shows significant (Mann-Kendall p-value < 0.05) long-term tendencies of -3.8 ± 1.9 % and -9.3 ± 3.8 % century^{-1} for annual and autumn precipitation, respectively, even though the annual trend is not significant by excluding the first decades from the evaluation. As the basin precipitation record is expected to be underestimated due to the rain-gauge snow undercatch, the monthly precipitation fields are subjected to a correction procedure which allows to derive the multiplicative correcting constant to be applied to the

basin annual precipitation series. The comparison between 1845–2016 yearly corrected precipitation and runoff records highlights current annual water losses of about 400 mm while the annual runoff coefficients exhibit a long-term significant decrease of -6.4 ± 1.0 % century^{-1}. This change in the hydrological cycle is mostly to be ascribed to the strong long-term reduction in annual runoff values (-11.8 ± 3.2 % century^{-1}) driven by increasing evapotranspiration due to both temperature increase and, likely, land-use changes.

1. Introduction

Alpine region is particularly prone to global warming, showing a significantly higher temperature trend than the Earth's average one. Indeed, the HISTALP database, one of the best archive of secular meteorological series in the world (e.g. Auer et al., 2007) gives evidence of a temperature increase of about 1.5 °C in the last 150 years, recorded both at low and high-elevation areas (Böhm et al., 2001; Brunetti et al., 2009). Beside temperature trend, also precipitation variability and changes in its seasonality over the Alpine region were documented in the scientific literature (e.g. Schmidli et al., 2002; Casty et al., 2005; Brunetti et al., 2006a).

The climate change poses a severe threat to the Alpine hydrological system, causing a significant pressure on the key role that Alps have for water storage and supply with potential impacts on economic activities, such as agriculture, energy and industrial production, also on downstream regions (Viviroli et al., 2006; Schaefli et al., 2007; EEA, 2009, Beniston, 2012; Fatichi et al., 2014).

To face this problem, it is crucial i) to investigate the spatio-temporal evolution of precipitation over Alpine areas on secular time scales, ii) to assess long-term areal precipitation records for the main Alpine catchments and iii) to compare them with the corresponding runoff records. The latter allows in fact to highlight the effect of temperature induced changes in the occurrence of solid and liquid precipitation and its seasonality, in the snow water equivalent, as well as in the contributions of evapotranspiration and melting glaciers on the water disposal.

High-resolution datasets of monthly precipitation have been recently produced over the Alpine region for example by Efthymiadis at al. (2006) for the period 1800–2003 at 10-min spatial resolution and by Masson and Frei (2016) for the period 1901–2008 at 5 km

resolution, while Isotta et al. (2014) provided a 1971–2008 daily dataset at 5 km grid spacing. High-resolution analyses of precipitation were also provided over smaller Alpine domains, such as by Brugnara et al. (2012) and Golzio et al. (2018) for the central European Alps, by Gyalistras (2003) for Switzerland and by Durand et al. (2009) for the French Alps. Among the gridding methods which have been proposed so far, the so-called "anomaly method" is one of the most applied approaches (e.g. New et al., 2000; Mitchell and Jones, 2005). All the gridding procedures aim at projecting the in-situ observations onto the cells of a regular grid, allowing to evaluate the climatic signal for a number of points which can be of several orders of magnitude larger than the number of the available rain-gauges. The long-term analyses performed on both monthly and daily scales revealed spatially heterogeneous trends in total precipitation and in statistical indexes over the Alps (e.g. Brunetti et al., 2006a; Scherrer et al., 2016; Pavan et al., 2018). Besides to spatial variability, trend slope and significance were found to be dependent also on the examined period, suggesting the need of continuous update for both present and past years (see e.g. Brugnara et al., 2012).

In this framework, we applied the anomaly method to reconstruct a 30-arc second resolution dataset of 1800–2016 monthly precipitation records for an area centred over the upper part of Adda river basin, an important water reservoir in the Central Alps for a wide portion of Northern Italy. This area is covered by a relevant number of long meteorological observations and it has one of the longest daily runoff records in Italy which has been recently recovered over the period 1845–2016. This record is presented and analysed (Ranzi et al., this issue) in the second part of the multi-century meteo-hydrological analysis for the Adda river basin of which this paper is the first part. The upper part of Adda river basin represents therefore a very interesting region to better investigate the response of Alpine water resources to climate variability and change.

The computed precipitation dataset constitutes an improvement to the state of the art for this area: it is based on a very dense observation database spanning more than two centuries and containing quality-checked and homogenized series retrieved from both national and extra-national sources, from new digitization activities and from the recent automatic station records, which allow to extend the reconstruction up to date and to improve the data coverage, especially at higher elevations. In the last decades in fact a relevant number of rain-gauges

was established in mountainous areas where observations are requested for both hydropower production and activities of prevention of natural hazards. The availability of new records allows to reduce the general difficulty in reconstructing the precipitation signal over mountainous regions which is mainly due to the uneven coverage of observations decreasing towards higher elevations, the low availability of secular station records and the heterogeneity of precipitation gradients due to the complex interactions between atmospheric circulation and the roughness of the surface (Haylock et al., 2008). Another relevant issue to be considered is the well-known rain-gauge undercatch, especially of solid precipitation, which could lead to significant precipitation underestimations in mountainous domains (Sevruk, 2009).

The paper aims at presenting the dataset, at assessing the robustness of the gridding method in relation to the development of the station network and at describing the multi-century record of areal precipitation extracted from the monthly gridded fields for the upper Adda river basin. This record is then analysed to investigate the trends and variability in precipitation regime over the basin and to perform the comparison with the 1845–2016 runoff coefficient. The monthly database allowed to extend the precipitation reconstruction back to 1800 and the availability of total areal precipitation values for the basin over the first half of the 19th century could represent a helpful proxy-data to estimate runoff even when this information was not yet collected. All the analyses were performed on monthly resolution due to the low availability of daily precipitation data before 1951, which are still stored in hardcopy yearbooks.

2. Materials and Methods

2.1 The study area

This study focuses on an area centred on the upper part of the Adda river catchment (45.6°–46.7°N and 8.8°–10.7°E, Figure 1b). This area will be called thereafter "study domain", while the word "study basin" will be used to refer to the upper basin of the Adda river (the region bordered by the yellow line in Figure 1b), which is one of the main tributaries of Po river. The study basin includes an area of 4508 km^2 mostly located over the southern Alpine ridge in Lombardy, from the Rhaetian Alps to the Lake Como outlet in Lecco. The region is characterized by a very heterogeneous orography, which is predominated by the mountain

environment and includes some of the main glaciers of the Central Alps contributing, to limited extent, to the annual hydrological cycle of the study basin. A more detailed description of the study basin and of the water uptake regulation is provided in the companion paper (Ranzi et al., this issue).

2.2 The observation database

The database used to compute the study domain gridded dataset of 1800–2016 monthly precipitation series was set up by starting from the collection of monthly precipitation records performed by Crespi et al. (2018) which is mainly based on the archive of the former Italian Hydrographic Service (Servizio Idrografico, SI). Two different data collection approaches were used for the study domain (Figure 1b and red bordered region in Figure 1a) and for the outer area (Figure 1a).

The data availability over the study domain was improved by:

- including the Trentino-Alto Adige/Südtirol monthly records provided by the digitization project "Before 1921" (https://before1921.wordpress.com). These new data allowed to extend into the past 37 series previously available only from 1921 and to add two new records;
- digitizing new data from the yearbooks of the former SI (Servizio Idrografico, 1920; 1925; 1957). 28 series previously available only from 1951 were extended in the past. The records to digitize were selected by prioritizing the stations of the study domain with the longest time coverage and located at the highest elevations;
- performing a new download of all the precipitation records available for the study domain from Meteotrentino (updated to April 2017) and from MeteoSwiss (updated to September 2017). In case of available homogenized Swiss station series, they were preferred to the original versions;
- collecting all precipitation records provided by the mechanical and automatic stations of the Regional Environmental Protection Agency (ARPA) and the Geological Monitoring Centre (CMG) of Lombardy. The records of automatic stations were merged with those of the mechanical ones allowing to overcome the general fragmentation of records occurring at most Italian sites since the 1980s, due to the

transition from manual to automatic monitoring systems as well as the transition of the national rain-gauge network from SI to the Italian regions.

The precipitation station records inside the study domain are indeed the most relevant ones for the present work. However, no data are available over this area before the 1860s and the station coverage remains quite sparse over the following decades too. In order to improve the observation availability and to get reliable information about the climate evolution also for the ancient years, it was necessary to include in the data collection activities a wider region around the domain. For this region, all the longest series available from the monthly homogenized archives of MeteoSwiss and HISTALP (Auer et al. 2007) were considered together with the homogenized versions of some of the longest Italian precipitation records starting in the 18^{th} century or in the first half of the 19^{th} century (Brunetti et al., 2006b). These stations allow the evaluation of the precipitation signal for the study domain in the earliest period, while they provide a marginal contribution to the reconstruction in the following decades when the station coverage over the study domain increases.

The collected series were checked for quality and homogeneity, except for the ones derived from already quality-controlled and homogenized archives. The quality-check procedure was performed, as described in Crespi et al. (2018), by comparing each measured series with a simulated one by means of neighbouring observations. High errors in the comparison allowed to remove gross errors such as outliers, spurious sequences of null values and digitization oversights. The series showing high deviations from the reconstructions and those with less than 10 years of data were definitely discarded from the database. When more than one source was available for the same site, the record with the longest time coverage and/or the highest quality was retained.

The homogeneity was then evaluated by applying the Craddock test (Craddock, 1979) on more than 400 monthly series with at least 20 years of data and, in case of relevant breaks, the homogenization was performed. 125 series containing on average 85 years of data were homogenized by identifying more than 300 breaks.

The final monthly database contains 338 precipitation series inside the study domain and 102 inside the study basin, while the stations outside the study domain with data before 1861 are 54, with 10 stations having data before 1811, represented as black points in Figure 1a. 120

178 series contain more than 120 years of data and 14 out of them are located within the study
179 domain. The time evolution of the data availability for the study domain and study basin is
180 shown in Figure 2. The first stations operating inside the study domain started in 1861 and
181 in 1873 inside the study basin. The station density increased significantly from the beginning
182 of the 20th century thanks to the contribution of the new meteorological network managed by
183 SI. After the difficulties due to the World War II, the greatest station availability is reached,
184 especially from 1951 to the end of the century when SI was closed and the Italian national
185 network was fragmented into regional and sub-regional Agencies with the concurrent
186 transition from the mechanical to automatic monitoring systems.
187 The inter-station distance, i.e. the mean distance between each station and the closest one,
188 over the whole area spanned by the database decreases gradually from about 150 km in the
189 first decade, when less than 10 stations are available, to about 60 km in 1860 when 53 rain-
190 gauges were operating and to 25 km in 1900 with more than 250 records. During the 20th
191 century this value reduces further reaching about 8 km within the study domain in the decades
192 of maximum data availability (1951–2000).
193 The rain-gauge density varies significantly over the years also on altitude ranges. Most of the
194 ancient sites are located at low elevations and the distribution gradually becomes more
195 homogeneous over all the elevation bands in the 20th century. Despite of the increment of
196 data availability for the highest elevations, the coverage of in-situ data is still low or even
197 missing for a relevant fraction of the grid cells located above 2000 m a.s.l. which are about
198 30% of study area grid cells.
199 *2.3 The interpolation scheme: from rain-gauge network to gridded records*
200 The gridded dataset of 1800–2016 monthly precipitation records over the study domain was
201 reconstructed on a 30-arc second resolution digital elevation model (DEM) by means of the
202 anomaly method. In this scheme the precipitation signal is reconstructed by superimposing
203 the spatial fields of monthly climatologies and the spatio-temporal fields of relative
204 anomalies. The two fields are computed separately and the final monthly estimate is obtained
205 by their product.
206 The monthly precipitation climatologies were constructed over the 1961–1990 period
207 corresponding to the 30 years of maximum data availability. The station monthly normals

were computed after completing the gaps of the series over the reference period and the resulting data density is on average one station per 53 km^2. They were then interpolated onto the DEM by means of a Local Weighted Linear precipitation-elevation Regression (LWLR) as described in Crespi et al. (2018). In LWLR the precipitation-elevation relationship is allowed to change for each grid cell. In fact, precipitation-elevation relationship is estimated for each 30 arc-second grid cell of the domain by choosing the most appropriate set of stations taking into account the topographic similarities between the stations and the grid cell itself, in terms of radial distance (rad), vertical distance (h), slope steepness (st), slope orientation (facet) and distance from the sea. In order to take into account the actual spatial scales at which the interactions between atmospheric circulation and orography are expected to occur, a smoothed DEM version was used where the terrain details are reduced but retaining the original horizontal step of 30 arc-second (Daly et al., 2002; Foresti et al., 2018; Crespi et al., 2018).

To compute the anomaly fields the station monthly records over the period 1800–2016 were converted into monthly relative anomalies, i.e. the ratio to their corresponding 1961–1990 normals, and they were interpolated over the DEM by means of a weighted averaging scheme. In this method, the relative anomaly for a certain month and grid cell is defined by the weighted average of the surrounding station anomalies whose weights are expressed as the product of Gaussian functions depending on radial and vertical distance from the target point (Brunetti et al., 2012). The halving distance of the radial weight was defined year-by-year according to the evolution of data availability over the whole period. In particular, it corresponds to the mean radius of the circle centred on the grid cells and containing at least three stations with valid observations. The value rapidly decreases from about 200 km during the earliest years to about 20 km in 1900 and further to 10 km after 1951 up to present. This approach allowed to exploit the fine-scale information provided by the period of dense data coverage and to include the available records on a larger area when stations are sparser (Brunetti et al., 2012). The halving factor for the weight of elevation difference was set to 2250 m over the whole period on the basis of a minimization error procedure. Since it is relatively high, the station weights are mainly defined by the nearness to the considered cell.

The 1800–2016 monthly precipitation records in absolute values over the grid were finally obtained as the product of the 1961–1990 monthly climatologies and the interpolated series of monthly anomalies. As examples of the resulting fields, in Figure 3 the precipitation distribution for the months featuring the highest total areal monthly precipitation sum on the study basin over each 40-year subperiods from 1861 to present are reported together with the available station records. The figure highlights also the gradual increase of data coverage over the study domain which passes from 8 stations for September 1882 to almost 200 stations in October 1960.

The 1800–2016 monthly areal precipitation record of the upper part Adda river basin was obtained as follows:

$$q_t = \sum_j p_{j,t} \cdot S_j \cdot f_j \qquad (1)$$

where q_t is the areal precipitation for the time step t, $p_{j,t}$ is the precipitation reconstructed for the time step t at the grid cell j and S_j and f_j are the cell area and the fraction of cell belonging to the basin, respectively. In order to express the precipitation record in millimeters, the computed values were finally normalized by the basin total surface.

2.4 Validation of gridded data and basin precipitation series

The accuracy of the climatologies was assessed by reconstructing in leave-one-out (LOO) approach the 1961–1990 monthly normals of the 338 stations inside the study domain, i.e. by excluding the observation under reconstruction in order to avoid self-influence. The same LOO reconstruction was also applied on the monthly anomaly series of the 338 stations within the study domain in order to evaluate the agreement between the modelled anomalies and the observed ones. The errors were evaluated in terms of mean error (BIAS), mean absolute error (MAE), mean absolute percentage error (MAPE) and root mean square error (RMSE).

However, the reconstruction errors of monthly records could be computed only from 1864, because no record is available for the study domain until 1861 and the data coverage before 1864, when most Swiss rain-gauges started operating, is not enough to provide a significant evaluation of the reconstruction ability at station sites. In order to evaluate the reconstruction accuracy of the anomaly gridding procedure also over the early years, an iterative procedure was performed. The period 1801–1950 was divided in 30 consecutive 5-year intervals and

the 1951–2000 monthly anomalies of all the stations in the study domain were iteratively reconstructed in LOO approach by considering only the records of the stations operating in each 5-year subperiod. The 1951–2000 period was chosen as reference as it corresponds to the years of best station coverage. The same halving distance coefficient, already computed for each year whose data availability is considered (see section 2.3), was used and whenever a station record selected for the reconstruction did not cover the period 1951–2000 the anomalies of the nearest available station were used in order to prevent the reconstruction from being biased by the missing data. The reconstruction errors were computed by comparing the measured 1951–2000 monthly anomalies of each station in the study domain with the corresponding simulated series obtained by varying the data coverage.

The same procedure was applied also to evaluate the uncertainty evolution of the monthly basin precipitation record in relation to the rain-gauge coverage variation over the study period. Since the actual monthly total precipitation series over the basin is unknown, the estimated values over the 1951–2000 period of best data availability were considered as reference since they are expected to be characterized by the highest robustness. The 1951–2000 monthly basin precipitation record was then iteratively reconstructed by computing the monthly anomaly fields only from the data of the available stations in each 5-year subperiod from 1801 to 1950. At each iteration, the gridded dataset was rescaled to absolute values by means of the 1961–1990 climatologies and Eq. 1 was applied to get the areal precipitation estimates which were compared to the reference one. In particular, MAPE values were computed for each iteration as follows:

$$MAPE_i = \frac{1}{T} \cdot \sum_{t=1}^{T} \frac{|\tilde{q}_{t,i} - q_t|}{q_t} \cdot 100 \qquad (2)$$

where $\tilde{q}_{t,i}$ is the simulated basin precipitation for time step t by considering the station availability in subperiod i, q_t is the reference precipitation value at time t, T is the total length of the series and t runs from January 1951 to December 2000.

3. Results and Discussion

3.1 Climatologies, anomalies and precipitation records

The error values of 1961–1990 monthly climatology reconstruction are listed in Table 1. BIAS is almost null in all months with a slight underestimation in summer. Despite the lowest

MAE values, which are mainly due to the drier conditions, the model is affected by the greatest uncertainty in winter, when MAPE reaches the maximum in January (16%). The greater MAPE in winter could be partly ascribed to the difficulties in measuring the contribution from solid precipitation in high-elevated areas. The wind-induced undercatch is in fact one of the main causes of precipitation underestimation at mountain sites, which are mostly exposed to intense winds and snowfall events (Sevruk et al., 2009).

As regards the annual precipitation climatology (Figure 4), the mean annual precipitation normals for the study domain and the study basin are 1314 mm and 1296 mm, respectively. The driest area is located over the North-Eastern part of the study domain along the Venosta Valley where a rain shadow effect occurs leading to less than 500 mm $year^{-1}$, while the highest precipitation values occur over the western portion of the study domain over the Como Prealps and the Canton of Ticino with annual maxima exceeding 2000 mm, especially around the San Bernardino Pass. Other wet conditions are evident over the Orobian Alps, South of the basin, with annual totals ranging between 1600 and 2000 mm, while the innermost part of Valtellina is characterized by lower precipitation values, especially around Sondrio, where annual totals are below 800 mm $year^{-1}$. A similar pattern is also evident along the course of Oglio river flowing South-East of the Adda basin into Lake Iseo where annual totals decrease of about 25% with respect to surrounding areas.

The driest conditions occur during winter (DJF) over the entire area, with less than 100 mm $season^{-1}$ over wide portions of Valtellina, Grisons and Venosta Valley (Figure 5). Except for winter, the precipitation regime is almost invariant along the year, with slightly wetter conditions during summer (JJA) when they are mainly driven by convective phenomena enhanced by moist and warm Mediterranean air at low levels and drier and colder continental currents at higher levels. Considering the average over the grid cells of the study basin only, the precipitation normal is 170 mm in winter, 350 mm in spring (MAM), 410 mm in summer and 365 mm in autumn (SON), while the yearly cycle of monthly precipitation is characterized by the highest and rather constant contributions between April and November (~10% of yearly values), with other months accounting for about 5% of the yearly values.

As regards the accuracy of monthly anomaly reconstruction, by considering all the available data over the study period for each month, MAE ranges from 0.24 in December to 0.14 in May, confirming the greater difficulty in capturing winter precipitation.

Figure 6 reports the time evolution along the 1864–2016 period of average annual MAE and BIAS obtained over all the available station anomalies at each time step. The highest average MAE values occur at the beginning of the considered interval with maxima around 0.30 when they are mostly affected by the low data coverage, MAE gradually reduces over the following decades to about 0.20 and it decreases further to about 0.15 from the second half of the 20th century during the period of best data availability. A slight increment is evident in the last years, probably due to the decrease of updated data for the most recent period. The evolution of average BIAS is more regular and, except for the first two decades, it is almost null over the whole period.

By applying the iteratively procedure described in Section 2.4 also the influence of station density on the reconstruction accuracy was evaluated and the results are reported in Figure 7. The errors reduce significantly after 1861, when the first stations started operating inside the study domain, and the MAE distributions remain almost stable with median values around 0.2 from the beginning of the 20th century. It is worth noting that even if the coverage before 1860 leads to larger errors with medians around 0.4, there is no further decrease in performances even for the lowest data coverage of the first years, when very few stations enter in the interpolation.

The rather low reconstruction errors obtained over almost the whole investigated period are mainly due to the large spatial coherence of anomalies which allow to estimate a reliable climatic signal even when the data density is lower. The distribution of the correlation between the anomaly records of all the station pairs within the study domain as function of their distance shows in fact correlation values above 0.7 even for distances greater than 70 km.

The accuracy in reconstructing the secular monthly precipitation records in absolute values was also evaluated by converting the LOO station monthly anomalies into millimeters by means of the product for the corresponding LOO normals. The largest fraction of MAPE

values obtained by the comparison of the station simulations with observations over the 1864–2016 period ranges between 16% and 23% with about 20% as average value.

3.2 The 1800–2016 monthly areal precipitation record of the study basin

The 1800–2016 monthly areal precipitation record of the upper Adda river basin was computed by means of Eq. 1. The availability of the gridded precipitation dataset allowed to assess total precipitation falling on the study basin at any time step over the whole considered period. This information can be retrieved by means of the anomaly method and not directly from the absolute station records only: if the monthly precipitation fields were estimated by simply interpolating the monthly records of available stations, the study basin areal precipitation would be significantly underestimated, at least before 1951. The underestimation obtained by just interpolating the monthly observations before the 1860s is about 30% and it reduces to about 10% in the following years until 1900. After that the bias gradually decreases, even though it remains above 5% until 1951. This outcome reflects the fact that the station distribution before 1951 is biased towards low-level areas, where also precipitation normals are generally lower than at higher elevations. The anomaly method integrates the spatial precipitation gradients contained in the climatological fields allowing to avoid the bias due to the uneven station coverage in the resulting areal precipitation records for the study basin.

However, even though unbiased, the accuracy of this record varies over time. The error evolution, as obtained by means of the method described in the section 2.4, is summarized in Table 2. The MAPE (Eq. 2) computed on annual scale is about 10% for all the station coverages before 1855, it decreases to 7% by considering the data density of 1856–1860 and to 4% with the availability of 1861–1865 when the first stations inside the study domain started operating. The annual error reduces further to 2% with the station availability from 1881 and to 1% by taking into account the network coverage from 1921. The correlation coefficients between 1951–2000 simulated and reference precipitation records on annual scale show the same behaviour as MAPE, with values above 0.90 from 1861 availability onwards.

It is worth noting that the reconstruction from the few available data of the first decades is relatively robust and errors are constantly around 10% even when less than ten stations are

used for the interpolation. In order to assess the meaningfulness of the information on the study basin retrieved from these few stations all located outside the study domain, we extracted 1000 sets of 50 random values from a normal distribution with the same mean and standard deviation as the 1951–2000 annual precipitation series and the corresponding MAPEs were computed. The average error turns out to be about 20%, which proves the consistency of the estimated accuracy and gives evidence of the ability of the database to provide a reliable climate signal over the basin even for the most remote years. Very similar outcomes are depicted also at seasonal scale. The lowest agreement is pointed out for winter with MAPE of about 30% for the data availability of the first decades, when all the rain-gauges were located at low elevation, and it decreases below 5% only after 1910. For the other seasons, the reconstruction errors are below 5% already from 1881, when only 4 stations were operating inside the study basin, and they generally reach 2% by using the data distribution after 1910.

3.3 Variability and trends of the multi-century precipitation record of Adda basin

The 1800–2016 annual and seasonal precipitation records for the study basin (Figure 8) were analysed for long-term trends by performing the Theil-Sen test (Theil, 1950), while the trend significance was assessed by the Mann-Kendall test (Kendall, 1975). Considering a confidence level of 0.05, a significant negative annual trend of -51 ± 25 mm century^{-1} was pointed out, while, on seasonal scale, a negative tendency is depicted in all cases even though it turns out to be significant for autumn precipitation only with a loss of -40 ± 16 mm century^{-1}. These values correspond to a -3.8 ± 1.9 % and -9.3 ± 3.8 % century^{-1} decrease, respectively. The 1800–2016 negative trend is likely to be largely driven by the wet conditions characterizing the beginning of the 19th century. In addition, the earliest values are more affected by uncertainty which has to be considered in the trend evaluation. In fact, excluding the first decades the annual trend remains negative, but its p-value is above 0.05.

It is however worth considering that the long-term trend of the basin precipitation record could be slightly biased because of the changes over time of rain-gauge snow undercatch. A detailed discussion about this issue is provided in the following section, while trend estimations are performed without considering it also in order to allow the comparison with

412 other literature results which do generally not take into account the rain-gauge snow
413 undercatch.
414 In order to investigate the variability of precipitation over the basin on a finer time scale, a
415 running-trend analysis was performed on the 1800–2016 annual and seasonal records. The
416 Theil-Sen slopes and Mann-Kendall significances were computed on windows of increasing
417 width from 20 years up to the entire period spanned by the series and running from the
418 beginning to the end of the record. The running trend on annual values (Figure 9a) confirms
419 a negative long-term tendency which, however, assumes significance only if almost the
420 whole period is included in the evaluation. The most frequent trend values range from -10 to
421 +10 mm decade^{-1} but only a low fraction of the trends has p-values below 0.05, as shown by
422 the pixel size. A more relevant variability in precipitation regime is evident at shorter time
423 scales with a sequence of wetting and drying conditions, especially in the first half of the 20th
424 century. A high frequency variability was also pointed out for seasonal records (Figure 9b-
425 9e), while only the autumn series shows a significant drying tendency at long-time scale,
426 which persists even varying the beginning of the considered window. It is interesting to note
427 the strong negative trend in spring precipitation series starting from the 1910s that is evident
428 also for time windows longer than 50 years. This trend is due to the rather lower precipitation
429 values from the 1940s which correspond to a severe hydrological drought and which are
430 interrupted by a relevant increase in the 1970s (Figure 9c). After this decade, however, spring
431 precipitation returns to be rather low, with another very severe drought at the beginning of
432 the 21st century (see also Figure 8), and it shows significant negative trends even over 100-
433 year long periods starting around the 1910s. This spring trend is also highlighted by Brugnara
434 and Maugeri (2019).
435 *3.4 Comparison of basin precipitation and runoff series*
436 Before comparing the annual precipitation series of the study basin with the corresponding
437 runoff record (1845–2016), it is necessary to take into account the well-known problem of
438 rain-gauge snow undercatch, which could account for up to several tens of percents of the
439 measured values, especially at the high-level sites characterized by higher wind speed
440 (Sevruk, 1985; Richter, 1995; Frei and Schär, 1998). Ranzi et al. (1999) and Grossi et al.
441 (2017) showed that the underestimation of snow precipitation for a rain-gauge network in an

area including also the Adda river basin, could range between 30% and 70% depending on the location, wind velocity and instrument type.

Even though well-known, the problem of snow undercatch is very difficult to address as it is extremely site-dependent and relevant amount of station metadata and meteorological information, especially wind speed, are required to punctually provide reasonable evaluations of the undercatch. For this reason, most climatologies and precipitation analyses are performed without applying any correction at station level (e.g. Frei and Schär, 1998; Isotta et al., 2014; Crespi et al., 2018; Pavan et al., 2018): corrections which are not representative of the specificities of each station location could in fact introduce significant local errors reducing the accuracy of the interpolated fields.

In order to take anyway into account the rain-gauge snow undercatch at basin scale in the comparison with the annual runoff series, we tried to evaluate the entity of this systematic bias on the annual basin precipitation series. To do this, we need to consider the different issues affecting this evaluation: i) the snow undercatch correction should be applied only to the solid fraction of precipitation which has to be identified on the basis of the temperature of each grid cell; ii) the increase of temperature over the past decades caused a reduction of the snowfall events in some elevation bands and the consequent snow undercatch decrease along time introduces a spurious positive trend in total measured precipitation amount; iii) since the stations located at low elevation and in the inner valleys (i.e. where the solid precipitation amount and/or wind exposure are lower) are less affected by snow undercatch, its impact on the basin precipitation series varies in time, driven by temporal evolution of the spatial distribution of available stations: in the early period, for which anomalies are reconstructed from only low-level stations, the undercatch is less relevant.

In order to take into account all these issues, we firstly applied to each grid-point monthly precipitation value of the 1951–2000 period, i.e. the period with maximum data availability, the correcting algorithm proposed by Eccel et al. (2012) and also used by Grossi et al. (2017) for the Adda river basin. In this scheme, a correction factor of 1.5 is introduced to increase the precipitation likely occurring in solid form (with monthly average temperature $T \leq 0$ °C) while a linearly temperature-dependent correction is applied for precipitation likely occurring in mixed form (with monthly average 0 °C < T < 2 °C). The gridded monthly temperature

472 records we used in this procedure were computed by applying to temperature observations
473 the same anomaly procedure described for precipitation (Brunetti et al., 2012), exploiting the
474 high-resolution temperature climatology published by Brunetti et al. (2014) and an improved
475 version of the temperature time series presented in Brunetti et al. (2006b). The average ratio
476 between the corrected and uncorrected annual basin precipitation values turned out to be 1.11
477 which was applied as multiplicative coefficient to correct the latter series over the entire
478 1800–2016 period. The multiplicative coefficient was calculated over the 1951–2000 interval
479 even though temperature data are available for the entire study period because the station
480 network after 1950 provides the best representation of the whole elevation range of the study
481 domain. Before this year the availability of high-level rain-gauges decreases and, especially
482 in the first half of the 19th century, the database mainly represents low-level areas. The
483 precipitation anomalies of high-elevation grid cells for this period are derived from the
484 anomalies of low-elevation stations which are less affected by the undercatch bias: if we
485 corrected them directly, the correction would be overestimated since it assumes undercatch
486 contributions corresponding to high-elevation grid-cell temperatures.
487 A further limit of the correction procedure is that it was applied at monthly scale, but the
488 monthly average temperature provides only a rough estimation of the actual temperatures of
489 the days in which precipitation occurs.
490 The comparison with the annual runoff series was performed over the 1846–2016 period on
491 the basis of the hydrological year, i.e. from September to August, in order to take into account
492 the fraction of precipitation falling as snow during autumn and winter which is released
493 during the following snowmelt runoff in spring and summer. This is also the 12-month period
494 providing the highest correlation values between runoff and precipitation series, both with
495 and without snow correction. The mean annual difference between precipitation and runoff
496 proves the relevance of the correction: it turns out to range from about 300 mm in the first
497 years to about 400 mm in recent decades with a mean value over the whole period of 330
498 mm, which decreases to only 178 mm if the uncorrected precipitation series is considered.
499 Since the main mechanism explaining the water loss from the basin is evapotranspiration,
500 annual water losses below 200 mm seem to be strongly lower than expected. In fact, previous
501 literature studies applying the Penman-Monteith equation at specific sites in Adda basin (e.g.

Ranzi and Bacchi, 1998) and in nearby basins in Switzerland (Gurtz et al., 1999) suggest that the actual evapotranspiration over the study basin, whose mean elevation is 1591 m a.s.l., is currently expected to be around 400 mm per year.

Besides systematically underestimating the measured precipitation, the rain-gauge snow undercatch affects also the long-term precipitation trends due to the strong temperature increase occurring over the study period. In order to test the sensitivity of the snow undercatch to temperature, the correction algorithm was applied by both increasing and decreasing the grid-point temperatures by 1 °C and by comparing the resulting multiplicative coefficients. The temperature is found to have a small but significant influence on the long-term precipitation trend increasing the precipitation values at basin scale of about 1.5%-2.0% per °C of temperature increment. The low effect of temperature on the precipitation trend is also confirmed by deriving the grid-point precipitation anomalies only from the stations that are less affected by rain-gauge snow undercatch (i.e. stations below 500 m a.s.l. or in the inner valleys of higher elevation areas) and by comparing the annual basin precipitation series with the corresponding series obtained from the full database over the 1921–2016 period, which is the longest period in which high-elevation areas are still represented by a rather good station coverage. The annual differences between the basin precipitation series retrieved from all and low-level stations show a positive trend due to a slightly stronger decrease of the precipitation record obtained from the low-level stations. This positive trend is however rather small (17 mm century^{-1}, corresponding to slightly more than 1% century^{-1} of basin precipitation), even though the temperature trend in this period is rather strong (1.6 °C century^{-1}). Overall, these results suggest that temperature trend induces a positive bias of about 1% century^{-1} in long-term precipitation trend that is within the error of precipitation trend estimations.

The series of annual runoff coefficients, i.e. the ratios between annual runoff and corrected precipitation (Figure 10a), was then subjected to trend analysis. A strongly significant negative trend of -6.4 ± 1.0 % century^{-1} was pointed out over the whole period, also confirmed by the running trend graph (Figure 10b), where a significant negative trend is pointed out for almost all windows at least one century long. On shorter time scales

significant decreases are also evident for windows starting around 1850 and for time intervals beginning in the 1930s and in the 1980s and spanning 20-30 years.

Moreover, the windows starting at the end of the 19th century and spanning few decades exhibit an increasing tendency which can be explained by the corresponding positive trend of precipitation and resulting increased runoff. The negative trend of the annual runoff coefficient series is due to basin runoff decreasing stronger than basin precipitation. The basin runoff exhibits in fact a rather relevant reduction of -11.8 ± 3.2 % century^{-1} (Mann Kendall p-value strongly below 0.01) that is clearly stronger than the precipitation decrease, even if the hypothesis of the temperature-induced positive bias in precipitation record is considered. The TS trends in the 1846–2016 series of annual precipitation, runoff and runoff coefficient based on the hydrological year are summarized in Table 3, in both absolute and relative terms.

The decrease of the runoff coefficient series seems to highlight long-term changes in evapotranspiration probably mainly induced by increasing temperature, as will be discussed more in detail in the companion paper by Ranzi et al. (this issue), focused on the 172-long time series of daily runoff. Another contribution to the variation of the evapotranspiration over the study basin could derive from changes in land use and coverage occurring over the study period, with the expansion of forests enhanced by the gradual decline of human communities and pastures over the mountainous areas (Guidi et al., 2014; Ranzi et al., 2017). It is also worth noting that the recent enhancement of glacier melting could slightly mask the actual long-term decrease in the runoff coefficient which, without the contribution from glacier melting, could be even more negative than observed. This effect has however to be considered together with the positive bias in measured precipitation due to the reduction of the rain-gauge snow undercatch.

4. Conclusions

The 1800–2016 monthly areal precipitation series for the upper part of the Adda river basin (Central Alps) was computed by means of the anomaly method and a quality-checked and homogenized database of monthly station records spanning more than two centuries and covering a wide area centred on the study basin. More specifically, the record was computed from a 30-arc second resolution grid of 1800–2016 precipitation series obtained by

561 superimposing the 1961–1990 Local Weighted Linear precipitation-elevation Regression
562 climatologies and the corresponding monthly anomalies interpolated by a weighted
563 averaging approach depending on station distance and elevation difference from the target
564 cell.
565 The temporal evolution of the reconstruction accuracy as well as of the robustness of the
566 areal precipitation estimates in respect to the variability in data coverage was assessed by
567 means of leave-one-out validation and sensitivity tests. The accuracy rapidly increases after
568 the first decades and rather low errors are obtained even for the years of sparse data coverage
569 thanks to the anomaly method which avoids significant underestimations in areal
570 precipitation occurring if the station values were interpolated directly.
571 Significant negative trends were found for the 1800–2016 annual (-3.8 ± 1.9 % century^{-1})
572 and autumn (-9.3 ± 3.8 % century^{-1}) areal basin precipitation records, even if the p-value of
573 the annual signal is above 0.05 if the first decades are excluded from the analysis.
574 The comparison of the annual basin total precipitation series with the corresponding runoff
575 series over the 1845–2016 period allowed to better investigate both records. For this period,
576 the negative trend of uncorrected and corrected precipitation is -41±34 mm century^{-1} and -
577 46±37 mm century^{-1} respectively, but none of them is significant at 5 % level.
578 Firstly, it allowed to discuss the contribution of rain-gauge snow undercatch to the annual
579 basin precipitation series and to apply a suitable correcting procedure which is needed to
580 explain unrealistic low annual losses (below 200 mm) resulting from the difference between
581 uncorrected precipitation and runoff. The comparison between runoff and corrected
582 precipitation provides current annual evapotranspiration estimates over the basin of about
583 400 mm, a value consistent with the results reported in literature for the Adda river and rather
584 similar Alpine basins.
585 Secondly, the precipitation-runoff comparison allowed to highlight a strong decrease in the
586 runoff coefficient series (-6.4 ± 1.0 % century^{-1}) due to a relevant reduction of annual runoff
587 of -11.8 ± 3.2% century^{-1}. The runoff variation is expected to be mainly determined by the
588 increase in evapotranspiration which is probably driven by both warming and changes in land
589 use and coverage. In addition, a small contribution to runoff could derive from the accelerated

590 melting of basin Alpine glaciers during the recent decades which could slightly reduce the
591 actual runoff losses.

592 **5. Acknowledgments**

593 Consorzio dell'Adda is acknowledged for having provided runoff data over the period 1946–
594 2016 and water level data before. We also thank all the providers of meteorological data,
595 especially ARPA and CMG for Lombardy, Meteotrentino and the Autonomous Province of
596 Bolzano for Trentino-Alto Adige/Südtirol and MeteoSwiss for Switzerland. Milan University
597 activities have been performed within IPCC MOUPA (Interdisciplinary Project for assessing
598 current and expected Climate Change impacts on MOUntain PAstures), developed within the
599 AGER Project, funded by Fondazione Cariplo.

600 **References**

601 Auer I, Böhm R, Jurkovic A, Lipa W, Orlik A, Potzmann R, Schöner W, Ungersböck M,
602 Matulla C, Briffa K, Jones P, Efthymiadis D, Brunetti M, Nanni T, Maugeri M, Mercalli L,
603 Mestre O, Moisselin J, Begert M, Müller-Westermeier G, Kveton V, Bochnicek O, Stastny
604 P, Lapin M, Szalai S, Szentimrey T, Cegnar T, Dolinar M, Gajic-Capka M, Zaninovic K,
605 Majstorovic Z and Nieplova E (2007). HISTALP – Historical instrumental climatological
606 surface time series of the Greater Alpine Region HISTALP. International Journal of
607 Climatology 27: 17–46. https://doi.org/10.1002/joc.1377

608 Beniston M (2012). Impacts of climatic change on water and associated economic activities
609 in the Swiss Alps. Journal of Hydrology 412: 291-296.
610 https://doi.org/10.1016/j.jhydrol.2010.06.046

611 Böhm R, Auer I, Brunetti M, Maugeri M, Nanni T and Schöner W (2001). Regional
612 temperature variability in the European Alps 1760–1998 from homogenized instrumental
613 time series. International Journal of Climatology 21: 1779–1801.
614 https://doi.org/10.1002/joc.689

615 Brugnara Y, Brunetti M, Maugeri M, Nanni T and Simolo C (2012). High-resolution analysis
616 of daily precipitation trends in the central Alps over the last century. International Journal of
617 Climatology 32: 1406–1422. https://doi.org/10.1002/joc.2363

618 Brugnara Y and Maugeri M (2019). Daily precipitation variability in the southern Alps since
619 the late 19th century. International Journal of Climatology. Accepted Author Manuscript.
620 https://doi.org/10.1002/joc.6034
621 Brunetti M, Maugeri M, Nanni T, Auer I, Böhm R and Schöner W (2006a). Precipitation
622 variability and changes in the greater Alpine region over the 1800–2003 period. Journal of
623 Geophysical Research, 111, 111, D11107. https://doi.org/10.1029/2005JD006674
624 Brunetti M, Maugeri M, Monti F and Nanni T (2006b). Temperature and precipitation
625 variability in Italy in the last two centuries from homogenised instrumental time series.
626 International Journal of Climatology 26: 345–381. https://doi.org/10.1002/joc.1251
627 Brunetti M, Lentini G, Maugeri M, Nanni T, Auer I, Böhm R and Schöner W (2009). Climate
628 variability and change in the Greater Alpine Region over the last two centuries based on
629 multi-variable analysis. International Journal of Climatology 29: 2197–2225.
630 https://doi.org/10.1002/joc.1857
631 Brunetti M, Lentini G, Maugeri M, Nanni T and Spinoni J (2012). Projecting North Eastern
632 Italy temperature and precipitation secular records onto a high-resolution grid. Physics and
633 Chemistry of the Earth, Parts A/B/C, 40–41: 9–22. https://doi.org/10.1016/j.pce.2009.12.005
634 Brunetti M, Maugeri M, Nanni T, Simolo C and Spinoni J (2014). High-resolution
635 temperature climatology for Italy: interpolation method intercomparison. International
636 Journal of Climatology 34: 1278–1296. https://doi.org/10.1002/joc.3764
637 Casty C, Wanner H, Luterbacher J, Esper J and Böhm R (2005). Temperature and
638 precipitation variability in the European Alps since 1500. International Journal of
639 Climatology 25: 1855–1880. https://doi.org/10.1002/joc.1216
640 Consorzio dell'Adda (2003). Gli effetti della regolazione sulle portate dell'Adda e sulle piene
641 del lago di Como. Vol. 12, Milano.
642 Craddock J (1979). Methods of comparing annual rainfall records for climatic purposes.
643 Weather 34: 332–346. https://doi.org/10.1002/j.1477-8696.1979.tb03465.x
644 Crespi A, Brunetti M, Lentini G and Maugeri M (2018). 1961-1990 high-resolution monthly
645 precipitation climatologies for Italy. International Journal of Climatology 38: 878–895.
646 https://doi.org/10.1002/joc.5217

Daly C, Gibson WP, Taylor GH, Johnson GL and Pasteris P (2002). A knowledge-based approach to the statistical mapping of climate. Climate Research 22: 99–113. https://doi.org/10.3354/cr022099

Daly C (2006). Guidelines for assessing the suitability of spatial climate data sets. International Journal of Climatology 26: 707–721. https://doi.org/10.1002/joc.1322

Durand Y, Laternser M, Giraud G, Etchevers P, Lesaffre B and Mérindol L (2009). Reanalysis of 44 Yr of Climate in the French Alps (1958–2002): Methodology, Model Validation, Climatology, and Trends for Air Temperature and Precipitation. Journal of Applied Meteorology and Climatology 48: 429–449. https://doi.org/10.1175/2008JAMC1808.1

EEA (European Environment Agency). 2009. Regional climate change and adaptation. The Alps facing the challenge of changing water resources. EEA Technical Report, 143 pp. https://doi.org/10.2800/12552

Eccel E, Cau P and Ranzi R (2012). Data reconstruction and homogenization for reducing uncertainties in high-resolution climate analysis in Alpine regions. Theoretical and Applied Climatology 110: 345–358. https://doi.org/10.1007/s00704-012-0624-z

Efthymiadis D, Jones PD, Briffa KR, Auer I, Böhm R, Schöner W, Frei C and Schmidli J (2006). Construction of a 10-min-gridded precipitation data set for the Greater Alpine Region for 1800–2003, Journal of Geophysical Research 111: D01105. https://doi.org/10.1029/2005JD006120

Fatichi S, Rimkus S, Burlando P and Bordoy R (2014). Does internal climate variability overwhelm climate change signals in streamflow? The upper Po and Rhone basin case studies. Science of the Total Environment 493: 1171-1182. https://doi.org/10.1016/j.scitotenv.2013.12.014

Foresti L, Sideris I, Panziera L, Nerini D and Germann U (2018). A 10-year radar-based analysis of orographic precipitation growth and decay patterns over the Swiss Alpine region. Quarterly Journal of the Royal Meteorological Society 144:2277–2301. https://doi.org/10.1002/qj.3364

675 Frei C and Schär C (1998). A precipitation climatology of the Alps from high-resolution rain-
676 gauge observations. International Journal of Climatology 18: 873–900.
677 https://doi.org/10.1002/(SICI)1097-0088(19980630)18:8<873::AID-JOC255>3.0.CO;2-9
678 Gyalistras D (2003). Development and validation of a high-resolution monthly gridded
679 temperature and precipitation data set for Switzerland (1951-2000). Climate Research 25:
680 55–83. https://doi.org/10.3354/cr025055
681 Golzio A, Crespi A, Bollati IM, Senese A, Diolaiuti GA, Pelfini M and Maugeri M (2018).
682 High-Resolution Monthly Precipitation Fields (1913–2015) over a Complex Mountain Area
683 Centred on the Forni Valley (Central Italian Alps). Advances in Meteorology, 2018, ID
684 9123814, pp. 17. https://doi.org/10.1155/2018/9123814
685 Grossi G, Lendvai A, Peretti G and Ranzi R (2017). Snow Precipitation Measured by Gauges:
686 Systematic Error Estimation and Data Series Correction in the Central Italian Alps. Water 9:
687 461. https://doi.org/10.3390/w9070461
688 Guidi C, Vesterdal L, Gianelle D and Rodeghiero M (2014). Changes in soil organic carbon
689 and nitrogen following forest expansion on grassland in the Southern Alps. Forest Ecology
690 and Management 328: 103–116. https://doi.org/10.1016/j.foreco.2014.05.025
691 Gurtz J, Baltensweiler A and Lang H (1999). Spatially distributed hydrotope-based
692 modelling of evapotranspiration and runoff in mountainous basins. Hydrological Processes
693 13: 2751–2768. https://doi.org/10.1002/(SICI)1099-1085(19991215)13:17<2751::AID-
694 HYP897>3.0.CO;2-O
695 Isotta FA, Frei C, Weilguni V, Perčec Tadić M, Lassègues P, Rudolf B, Pavan V, Cacciamani
696 C, Antolini G, Ratto SM, Munari M, Micheletti S, Bonati V, Lussana C, Ronchi C, Panettieri
697 E, Marigo G and Vertačnik G (2014). The climate of daily precipitation in the Alps:
698 development and analysis of a high-resolution grid dataset from pan-Alpine rain-gauge data.
699 International Journal of Climatology 34: 1657–1675. https://doi.org/10.1002/joc.3794
700 Haylock MR, Hofstra N, Klein Tank AMG, Klok EJ, Jones PD and New M (2008). A
701 European daily high-resolution gridded data set of surface temperature and precipitation for
702 1950–2006. Journal of Geophysical Research 113: D20119.
703 https://doi.org/10.1029/2008JD010201
704 Kendall MG (1975). Rank Correlation Methods. Griffin, London.

Masson D and Frei C (2016). Long-term variations and trends of mesoscale precipitation in the Alps: recalculation and update for 1901-2008. International Journal of Climatology 36: 492–500. https://doi.org/10.1002/joc.4343

Mitchell TD and Jones PD (2005). An improved method of constructing a database of monthly climate observations and associated high-resolution grids. International Journal of Climatology 25: 693–712. https://doi.org/10.1002/joc.1181

New M, Todd M, Hulme M and Jones P (2001). Precipitation measurements and trends in the twentieth century. International Journal of Climatology 21: 1899–1922. https://doi.org/10.1002/joc.680

Pavan V, Antolini G, Barbiero R, Berni N, Brunier F, Cacciamani C, Cagnati A, Cazzuli O, Cicogna A, De Luigi C, Di Carlo E, Francioni M, Maraldo L, Marigo G, Micheletti S, Onorato L, Panettieri E, Pellegrini U, Pelosini R, Piccinini D, Ratto S, Ronchi C, Rusca L, Sofia S, Stelluti M, Tomozeiu R and Torrigiani Malaspina T (2018). High resolution climate precipitation analysis for north-central Italy, 1961–2015. Climate Dynamics 1–19. https://doi.org/10.1007/s00382-018-4337-6

Ranzi R and Bacchi B (1998). Il bilancio idrologico nelle aree montane per la stima delle disponibilita idriche: alcuni problemi aperti. XXVI Convegno di Idraulica e Costruzioni Idrauliche, Catania 3: 347–358.

Ranzi R, Grossi G and Bacchi B (1999). Ten years of monitoring areal snowpack in the Southern Alps using NOAA-AVHRR imagery, ground measurements and hydrological data. Hydrological Processes 13: 2079–2095. https://doi.org/10.1002/(SICI)1099-1085(199909)13:12/13<2079::AID-HYP875>3.0.CO;2-U

Ranzi R, Caronna P and Tomirotti M (2017). Impact of climatic and land use changes on riverflows in the Southern Alps, in: “Sustainable Water Resources Planning and Management Under Climate Change”, E. Kolokytha, S. Oishi, R.S.V. Teegavarapu (Eds.), Springer Science+Business Media, Singapore: 61–83. https://doi.org/10.1007/978-981-10-2051-3

Ranzi R, Michailidi E M, Tomirotti M, Crespi A, Brunetti M and Maugeri M (2019). A multi-century meteo-hydrological climatology for the Adda river basin (Central Alps). Part II: daily runoff (1845-2016) at different scales. International Journal of Climatology, this issue, submitted.

Richter D (1995). Ergebnisse methodischer Untersuchungen zur Korrektur des systematischen Messfehlers des Hellmannniederschlagsmessers, Berichte des Deutschen Wetterdienstes, Vol. 194.

Schaefli B, Hingray B and Musy A (2007). Climate change and hydropower production in the Swiss Alps: quantification of potential impacts and related modelling uncertainties. Hydrology and Earth System Sciences 11: 1191-1205. https://doi.org/10.5194/hess-11-1191-2007

Scherrer SC, Fischer EM, Posselt R, Liniger MA, Croci-Maspoli M and Knutti R (2016). Emerging trends in heavy precipitation and hot temperature extremes in Switzerland. Journal of Geophysical Research Atmosphere 121: 2626–2637. https://doi.org/10.1002/2015JD024634

Schmidli J, Schmutz C, Frei C, Wanner H and Schär C (2002). Mesoscale precipitation variability in the region of the European Alps during the 20th century. International Journal of Climatology 22: 1049–1074. https://doi.org/10.1002/joc.769

Servizio Idrografico (1920). Osservazioni pluviometriche raccolte a tutto l'anno 1915. Volume II: Bacino Imbrifero del Po. Fascicolo I. Ministero dei Lavori Pubblici – Consiglio Superiore delle Acque, Roma.

Servizio Idrografico (1925). Osservazioni pluviometriche raccolte nel quinquennio 1916–1920. Pubblicazione numero 1 del Servizio Idrografico. Volume V: Bacino del Po, Roma.

Servizio Idrografico (1959). Precipitazioni medie mensili ed annue e numero dei giorni piovosi per il trentennio 1921–1950. Pubblicazione numero 24 del Servizio Idrografico. Fascicolo XII b, Roma.

Sevruk B (1985). Correction of precipitation measurements. Proceedings of Workshop on the Correction of Precipitation Measurements, Zurich, Switzerland, WMO/IAHS/ETH, 13–23.

Sevruk B, Ondrás M and Chvíla B (2009). The WMO precipitation measurement intercomparisons. Atmospheric Research 92: 376–380. https://doi.org/10.1016/j.atmosres.2009.01.016

Theil H (1950). A rank-invariant method of linear and polynomial regression analysis. I. Proceedings of the Koninklijke Nederlandse Akademie van Wetenschappen A53: 386–392.

765 Viviroli D, Dürr HH, Messerli B, Meybeck M and Weingartner R (2007). Mountains of the
766 world, water towers for humanity: Typology, mapping, and global significance. Water
767 Resources Research 43: W07447. https://doi.org/10.1029/2006WR005653

768 **Figures and Tables**

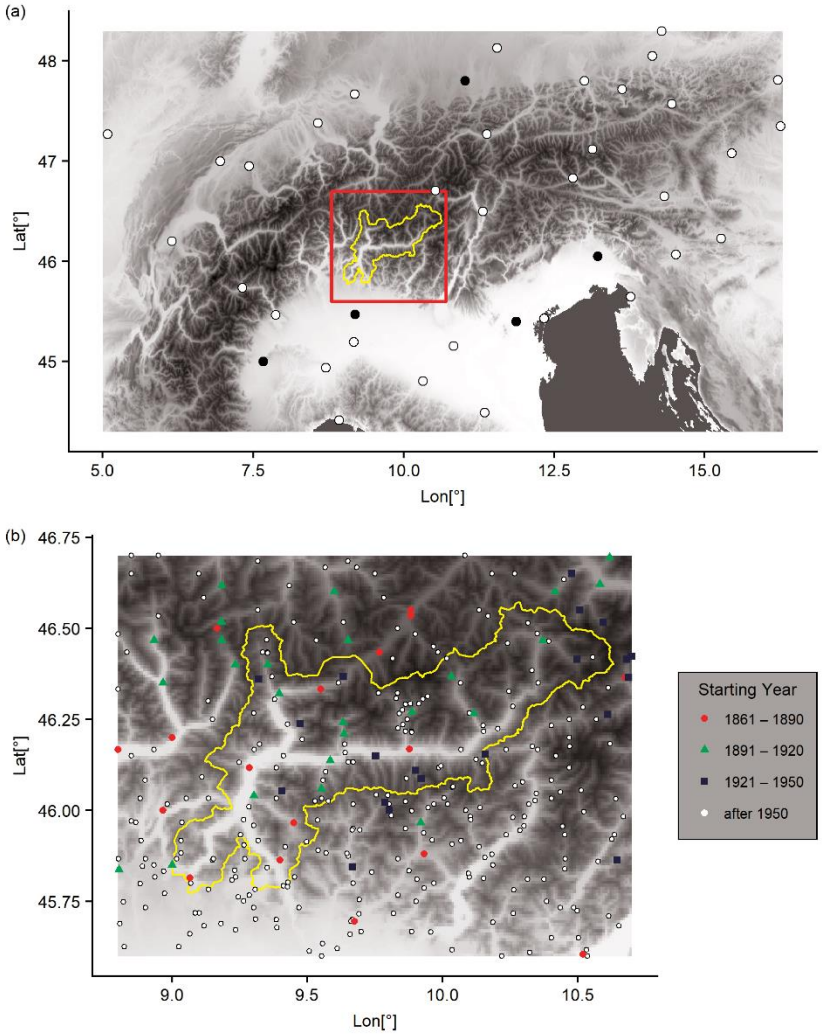

769 **Figure 1**: Spatial distribution of the available stations over (a) the larger area surrounding
770 the study
771 domain and (b) inside it. In panel (a) only the station series starting before 1861 are shown
772 with series starting before 1811 represented by black points, in panel (b) all the available
773 records are reported together with the corresponding starting year.

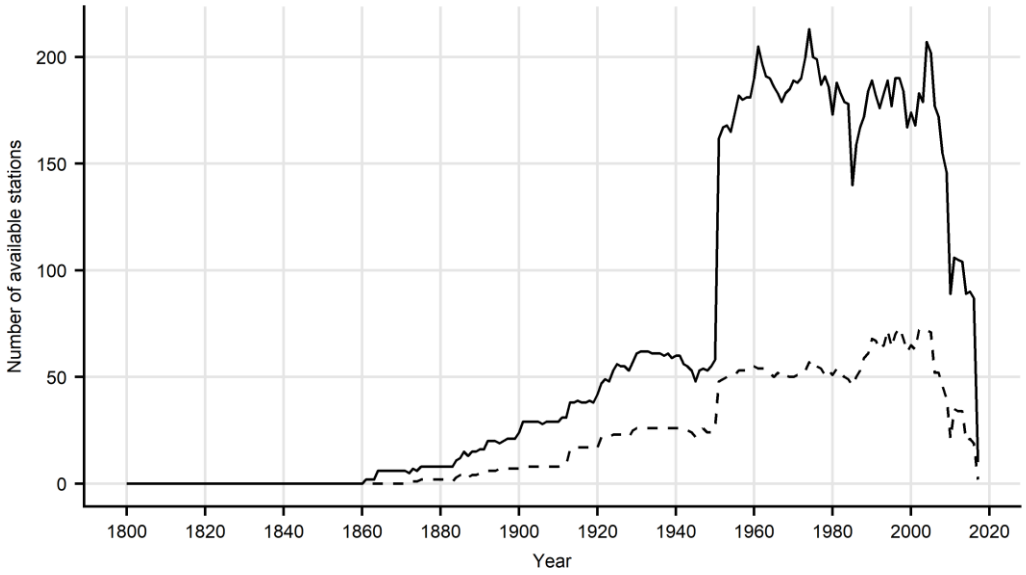

774 **Figure 2**: Availability of monthly records over the study domain (solid line) and the study
775 basin (dashed line).

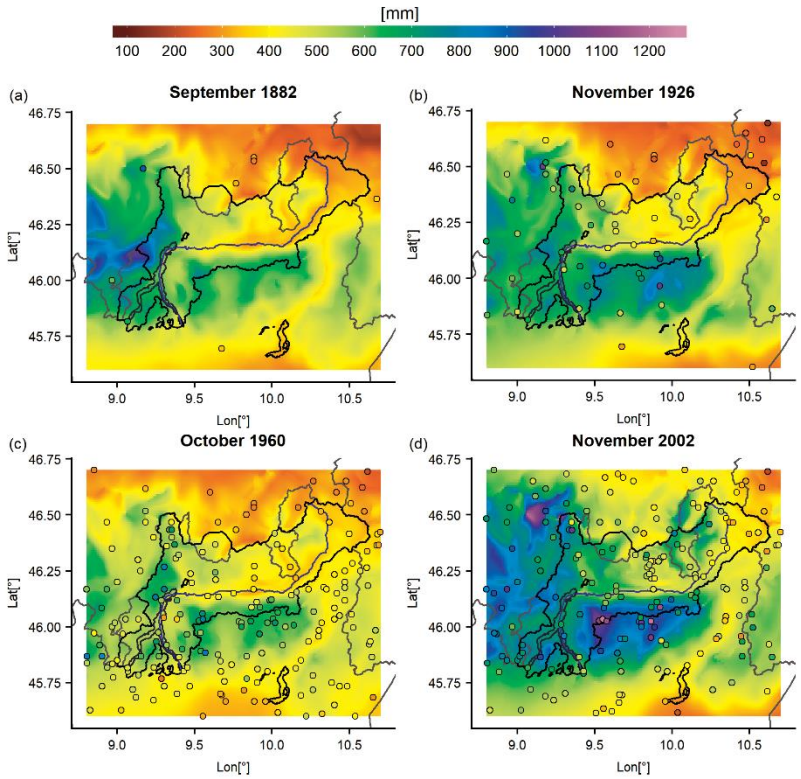

Figure 3: Monthly precipitation fields corresponding to the greatest total areal precipitation values over the study basin for the subperiods a) 1861–1900, b) 1901–1940, c) 1941–1980, d) 1981–2016. The points represent the monthly records at the available station sites.

MONTH	BIAS	MAE	MAPE [%]	RMSE
1	0.0	9.1	15.6	12.5
2	0.4	7.9	14.0	11.0
3	0.2	9.8	12.4	14.5
4	-0.1	13.7	12.1	20.5
5	-0.4	14.8	9.6	20.6
6	-0.3	12.6	9.3	16.6
7	-0.3	11.0	9.0	14.1
8	-0.5	11.1	8.0	14.8
9	-0.2	11.8	10.0	16.0
10	0.0	13.0	10.7	18.1
11	-0.2	13.6	12.3	20.3
12	0.2	8.0	14.3	11.6

Table 1: Monthly leave-one-out reconstruction errors of the 1961–1990 normals for the 338 stations included in the study domain. Except for MAPE, all the values are expressed in mm and BIAS is defined as the difference between simulation and observation.

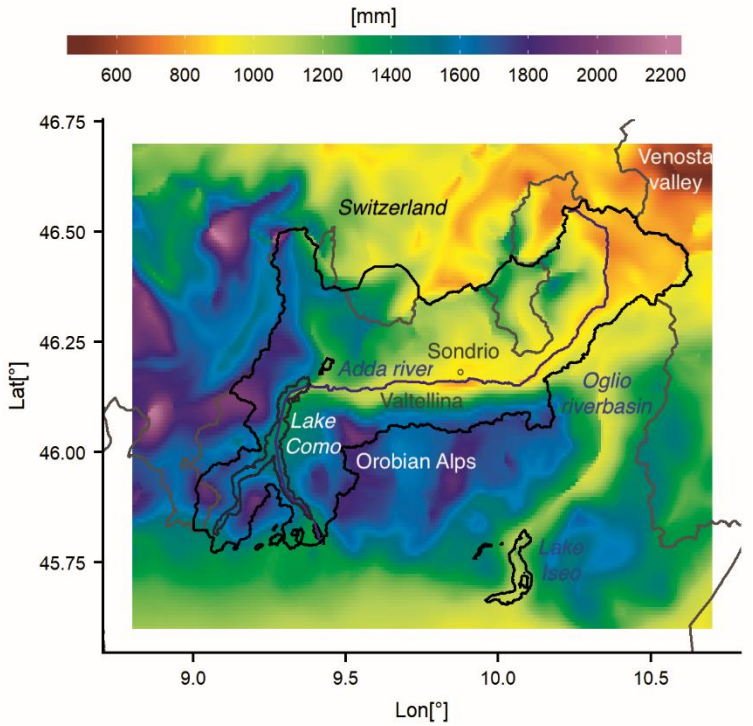

776 **Figure 4**: 1961–1990 annual precipitation climatologies.

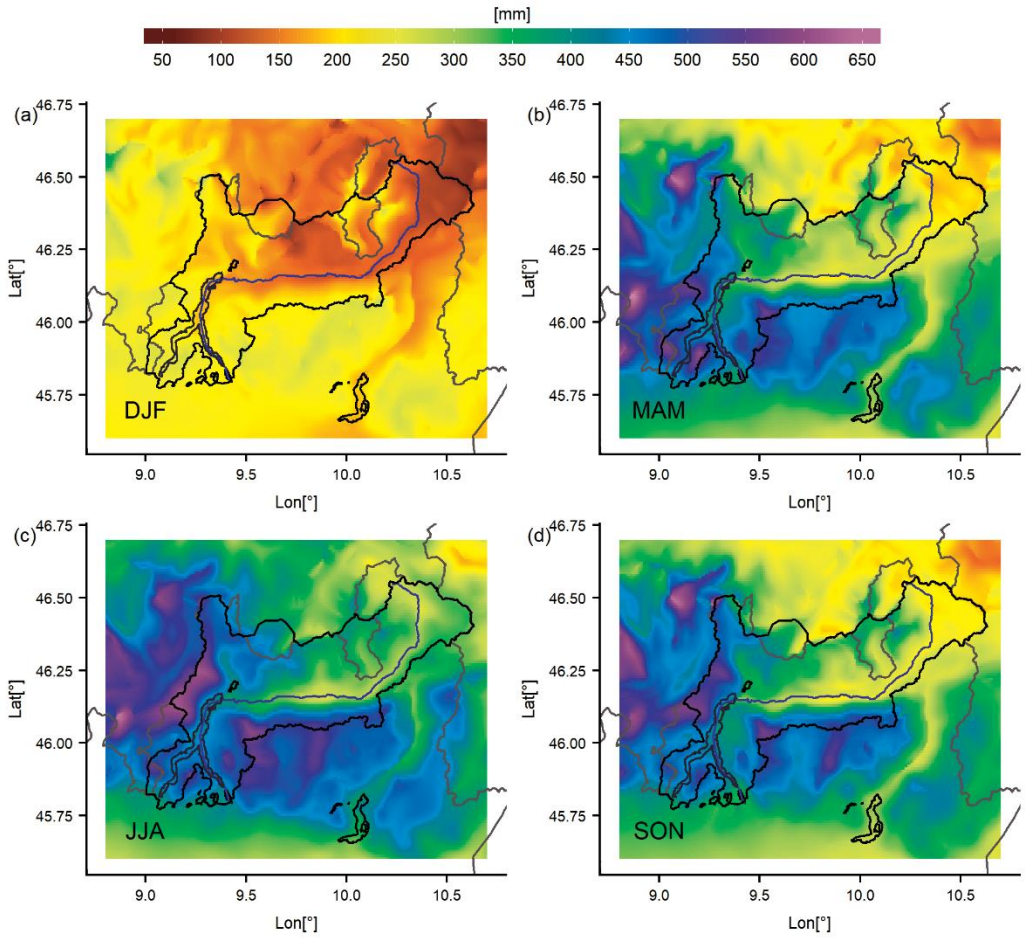

777 **Figure 5**: 1961–1990 seasonal precipitation climatologies.

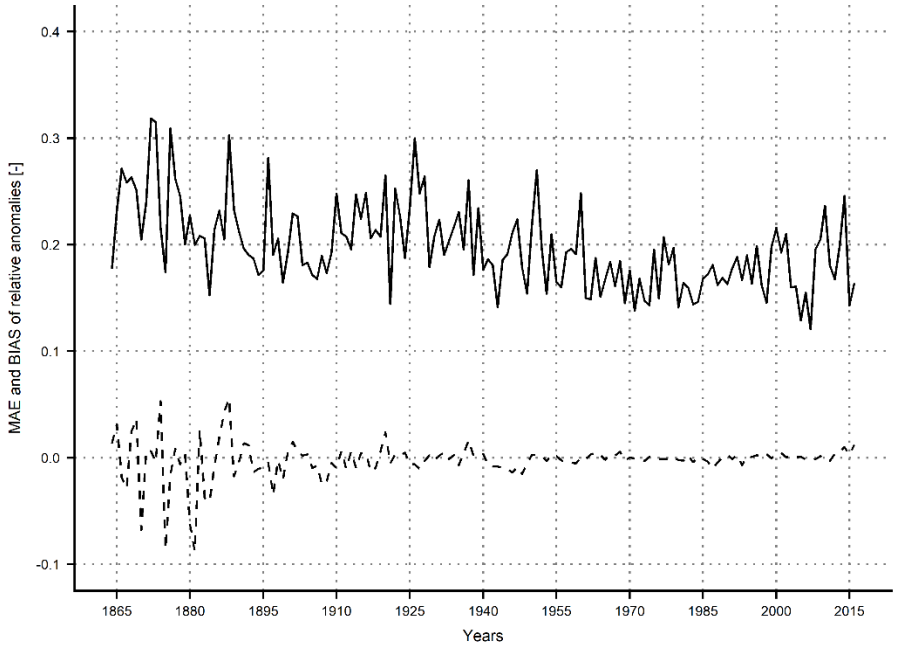

778 **Figure 6**: Evolution of annual MAE (solid line) and BIAS (dashed line) of leave-one-out
779 reconstruction of the 1864–2016 station monthly relative anomalies available inside the study
780 domain. The differences between simulated and measured station anomalies are considered.

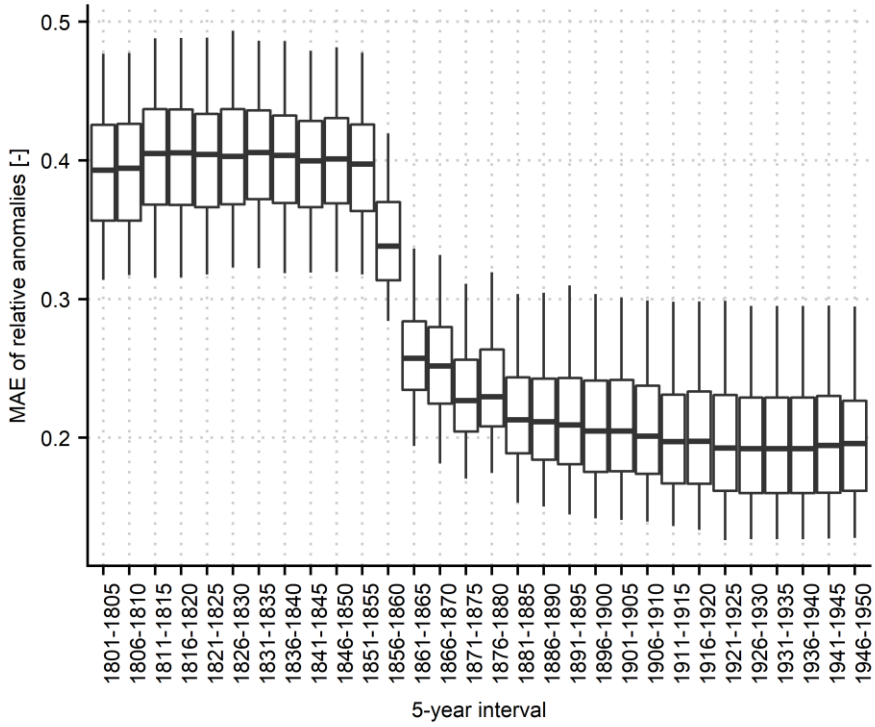

781 **Figure 7**: MAE distribution obtained from the reconstruction of the 1951–2000 monthly
782 anomalies of all the stations in the study domain by considering only the records from the

783 rain-gauges available in each 5-year subperiod from 1801 to 1950. The boxes represent the
784 inter-quartile range and the median is reported by the bold line; the whiskers represent the 5–
785 95% quantile range.

	YEAR		DJF	MAM	JJA	SON
5-YEAR DATA AVAILABILITY	MAPE [%]	r	MAPE [%]			
1801-1805	9.5	0.72	28.8	23.4	15.5	25.2
1821-1825	9.9	0.69	29.4	23.9	17.2	25.2
1841-1845	9.9	0.72	29.2	24.4	16.7	22.8
1856-1860	7.1	0.87	22.7	18.7	12.3	18.3
1861-1865	3.8	0.96	16.5	7.1	6.3	7.8
1881-1885	2.0	0.99	7.4	3.8	3.7	4.2
1901-1905	2.2	0.99	8.0	3.4	3.7	4.1
1911-1915	1.6	0.99	4.3	2.3	2.4	2.7
1921-1925	1.1	>0.99	3.4	1.6	1.7	1.9

Table 2: Annual and seasonal MAPE values of the reconstructed 1951–2000 total precipitation series by considering the data availability in some selected 5-year subperiods from 1801. For the annual simulations only, the correlation coefficients are reported too.

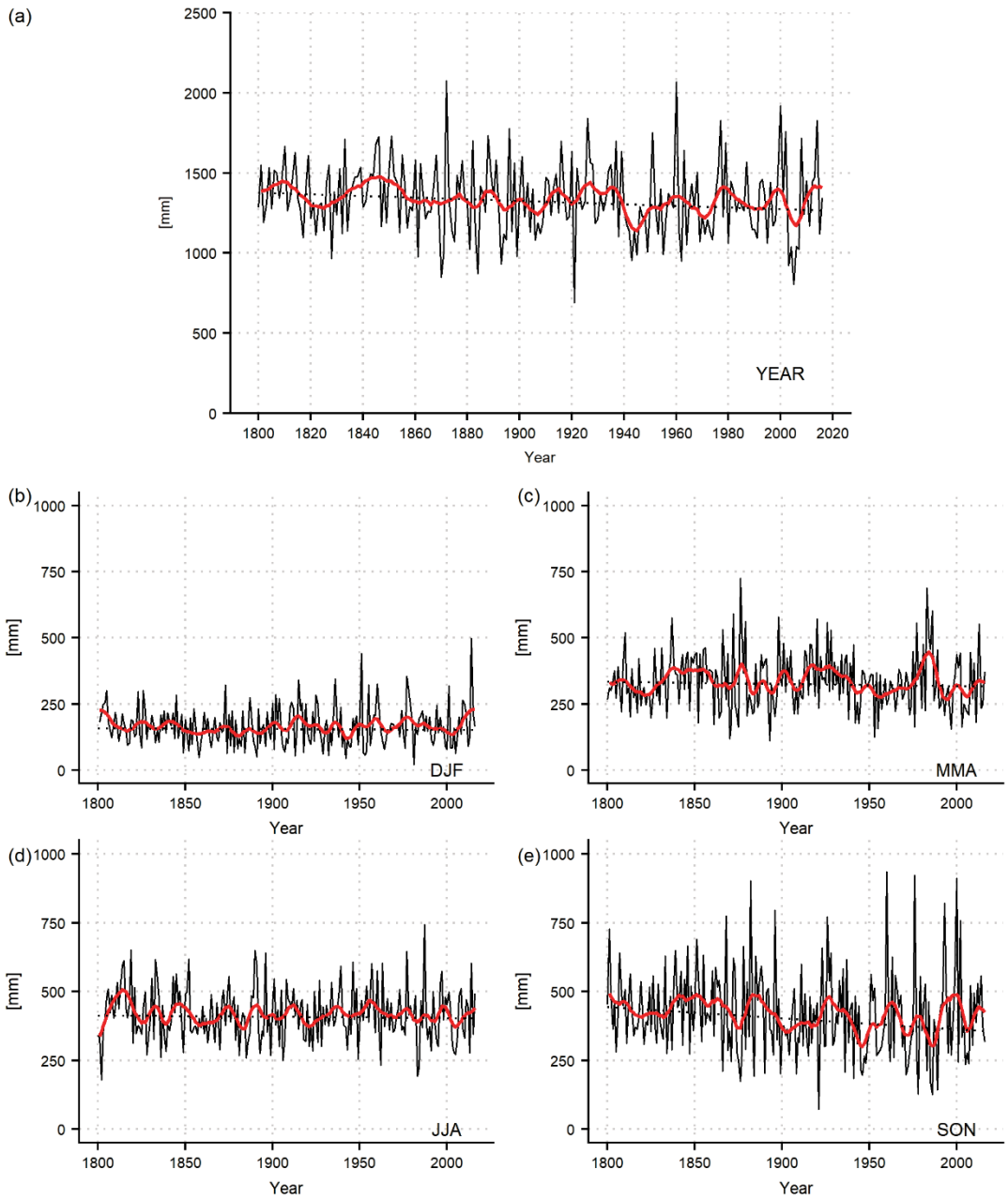

786 **Figure 8**: 1800–2016 annual and seasonal series of total precipitation of the upper Adda river
787 basin (solid black line) together with a 11-year centred Gaussian filter with 3-year standard
788 deviation (red solid line) and the Theil-Sen linear fit (dotted line).

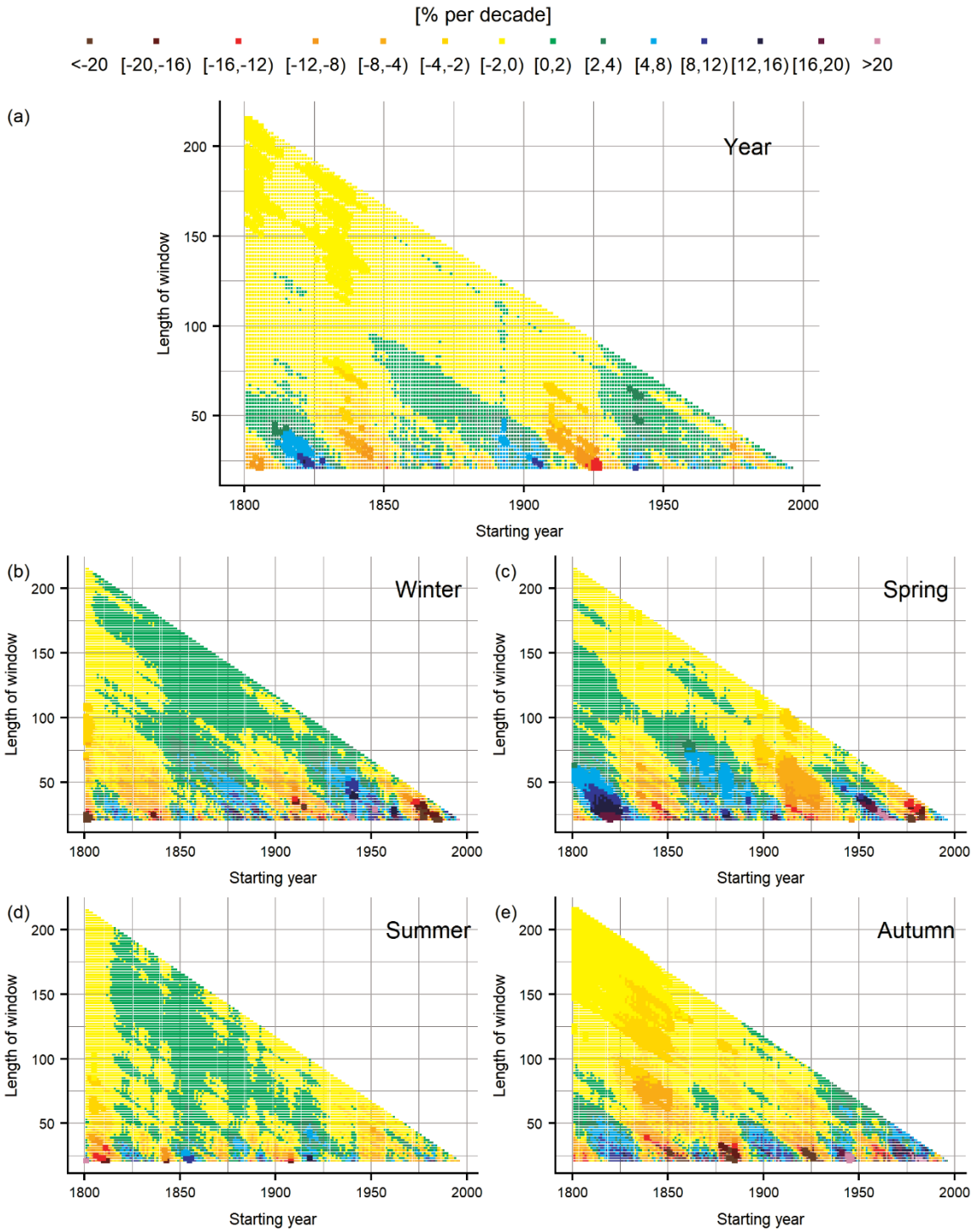

789 **Figure 9**: Running trend of annual and seasonal precipitation series. Trend values are
790 expressed by colours (green to purple positive and yellow to brown negative) while trend
791 significance is represented by the pixel size (larger pixels for Mann-Kendall p values <.05).

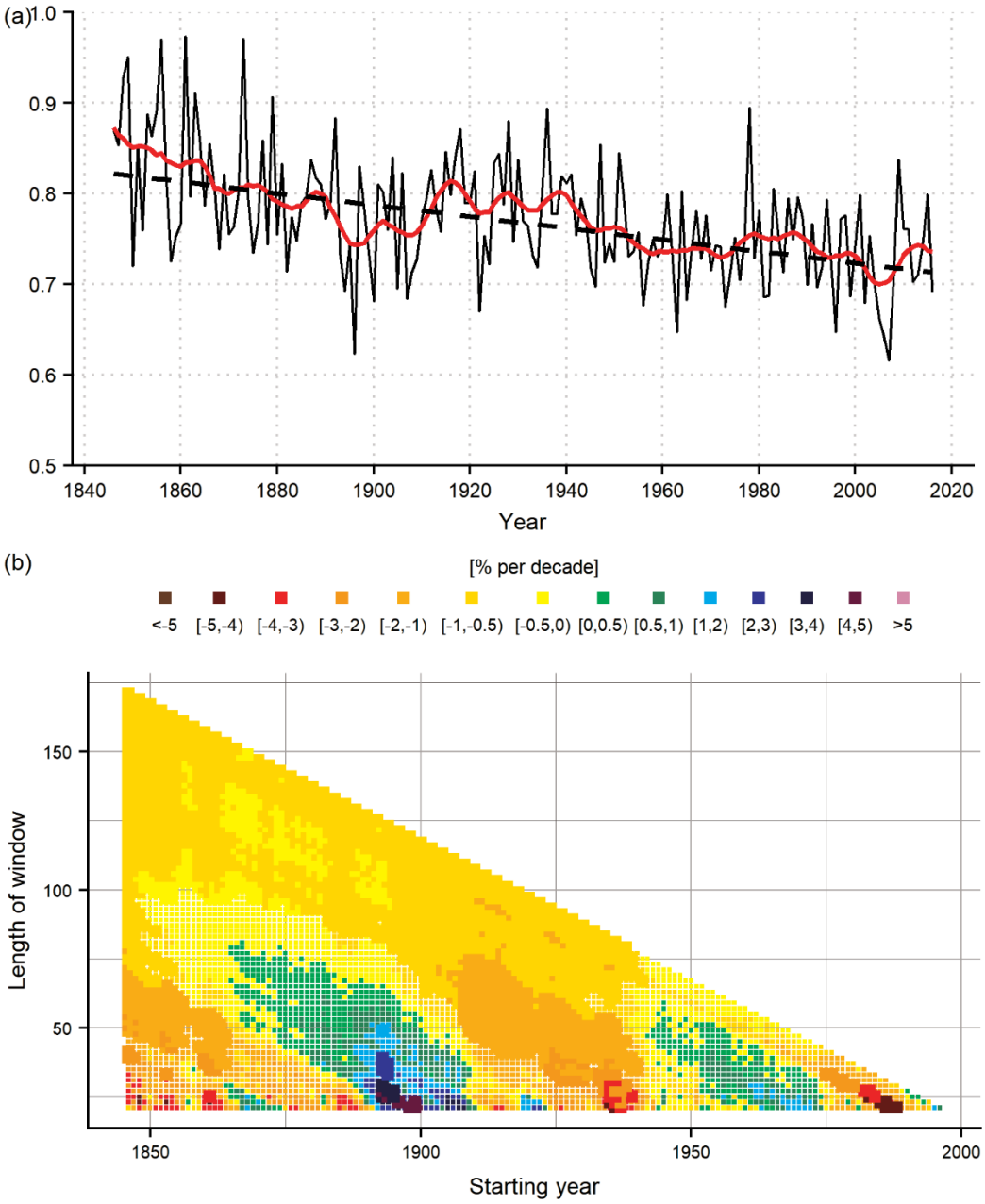

792 **Figure 10**: Temporal evolution of the annual (hydrological year) runoff coefficient: In panel
793 (a) the 1846–2016 series (black solid line) is shown together with a 11-year centred Gaussian
794 filter with 3-year standard deviation (red solid line) and the Theil-Sen linear fit (dashed line);
795 in panel b) the running trend is reported. Trend values are expressed by colours (green to
796 purple positive and yellow to brown negative) while trend significance is represented by the
797 pixel sizes (larger pixels for Mann-Kendall p values <.05).

	Annual Precipitation	Annual Runoff	Annual Runoff Coefficient
Absolute	- 46 ± 37 (mm century $^{-1}$)	- 136 ± 37 (mm century $^{-1}$)	- 0.064 ± 0.010 (mm/mm century $^{-1}$)
Relative	- 3.1 ± 2.5 (% century $^{-1}$)	- 11.8 ± 3.2 (% century $^{-1}$)	- 8.3 ± 1.3 (% century $^{-1}$)

Table 3: TS trend slopes obtained for the study basin annual precipitation, runoff and runoff coefficient over the period 1846–2016. The annual totals are based on the hydrological year, i.e. from September to August.